



CHALMERS
UNIVERSITY OF TECHNOLOGY

Strongly Stretched Protein Resistant Poly(ethylene glycol) Brushes Prepared by Grafting-To

Downloaded from: <https://research.chalmers.se>, 2026-06-20 22:41 UTC

Citation for the original published paper (version of record):

Emilsson, G., Schoch, R., Feuz, L. et al (2015). Strongly Stretched Protein Resistant Poly(ethylene glycol) Brushes Prepared by Grafting-To. *ACS Applied Materials & Interfaces*, 7(14): 7505-7515.
<http://dx.doi.org/10.1021/acsami.5b01590>

N.B. When citing this work, cite the original published paper.

Strongly Stretched Protein Resistant Poly(ethylene glycol) Brushes Prepared by Grafting-To

Gustav Emilsson,[†] Rafael L. Schoch,[‡] Laurent Feuz,[#] Fredrik Höök,[†] Roderick Y. H. Lim,[‡] and Andreas B. Dahlin^{*,†}

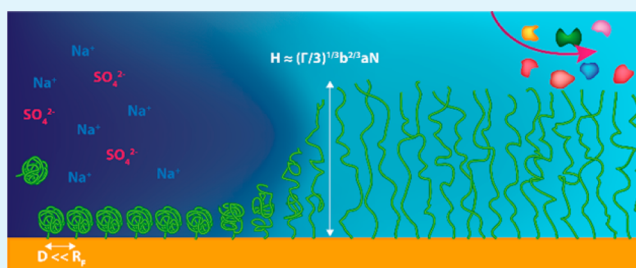
[†]Department of Applied Physics, Chalmers University of Technology, 41296 Göteborg, Sweden

[‡]Biozentrum and the Swiss Nanoscience Institute, University of Basel, 4056 Basel, Switzerland

S Supporting Information

ABSTRACT: We present a new grafting-to method for resistant “non-fouling” poly(ethylene glycol) brushes, which is based on grafting of polymers with reactive end groups in 0.9 M Na₂SO₄ at room temperature. The grafting process, the resulting brushes, and the resistance toward biomolecular adsorption are investigated by surface plasmon resonance, quartz crystal microbalance, and atomic force microscopy. We determine both grafting density and thickness independently and use narrow molecular weight distributions which result in well-defined brushes. High density (e.g., 0.4 coils per nm² for 10 kDa) and thick (40 nm for 20 kDa) brushes are readily achieved that suppress adsorption from complete serum (10× dilution, exposure for 50 min) by up to 99% on gold (down to 4 ng/cm² protein coverage). The brushes outperform oligo(ethylene glycol) monolayers prepared on the same surfaces and analyzed in the same manner. The brush heights are in agreement with calculations based on a simple model similar to the de Gennes “strongly stretched” brush, where the height is proportional to molecular weight. This result has so far generally been considered to be possible only for brushes prepared by grafting-from. Our results are consistent with the theory that the brushes act as kinetic barriers rather than efficient prevention of adsorption at equilibrium. We suggest that the free energy barrier for passing the brush depends on both monomer concentration and thickness. The extraordinary simplicity of the method and good inert properties of the brushes should make our results widely applicable in biointerface science.

KEYWORDS: poly(ethylene glycol), polymer brush, strongly stretched, inert, protein adsorption



INTRODUCTION

The possibility to create surfaces that are inert toward biomolecular adsorption is of vital importance in biointerface science¹ and in several technological applications.² For instance, in biosensors that are based on detecting molecular binding to a surface, specificity relies fully on chemical functionalization with a receptor in combination with a “non-fouling” background underneath to prevent nonspecific interactions^{3,4} (i.e., false positives). Also, implants and drug delivery vehicles are more likely to function in vivo if biomolecular adsorption on their surfaces is suppressed.⁵ In addition, patterning of proteins or cells on micro- and nanostructured surfaces that show material heterogeneity becomes straightforward if one of the materials can be rendered inert.⁶ Most approaches for making surfaces resistant to biomolecules are based on hydrophilic polymer brushes, i.e., polymers attached to the surface with such a high density that they are forced to extend into solution,⁷ thereby forming a layer with a thickness significantly higher than the characteristic end-to-end distance for the same polymer free in solution.

With a few exceptions,^{4,8–10} bioresistant coatings are practically always made of molecular chains with ethylene-

oxide units, the most common being simply poly(ethylene glycol) (PEG). PEG provides good performance while also being a cheap, nontoxic and well characterized polymer.¹¹ The main challenge for realizing an inert surface is to generate a brush with sufficiently high density.¹² One strategy is to use “grafting from”, i.e., to run the polymerization on the surface from a densely packed initiator layer.¹³ However, grafting-from methods not only tend to produce polydisperse brushes, but also require relatively complicated chemical synthesis, and conventional polymer characterization methods cannot be utilized. One alternative is to use block copolymers such as PEG chains bound at high density to a poly(lysine) backbone, which assembles on oxide surfaces by electrostatic interactions and forces the PEG branches to extend into solution.^{3,14} Another commonly used block copolymer consists of PEG chains bound to a poly(propylene oxide) backbone, which favors assembly to hydrophobic surfaces.^{15,16} However, depending on the surface these backbone constructs do not

Received: November 27, 2014

Accepted: March 26, 2015

Published: March 26, 2015

Table 1. Summary of Poly(ethylene glycol) Molecules Used, Properties of the Resulting Brushes Prepared by Grafting-to and Their Protein Resistance^a

molecular weight (kDa)	2	5	10	20	30
concentration for grafting in 0.9 M Na ₂ SO ₄ (g/L)	>2	>0.6	0.33	0.12	0.07
calculated Flory radius in water (nm)	4.0	7.0	10.6	16.1	20.5
saturated grafting density (nm ⁻²)	0.92 ± 0.068	0.54 ± 0.042	0.38 ± 0.036	0.19 ± 0.011	0.081 ± 0.023
height by SPR (nm)	6.50 ± 0.71	12.14 ± 1.05	23.56 ± 2.17	38.15 ± 4.06	28.77 ± 6.51
average height by AFM (nm)	-	15.4 ± 1.8	25.7 ± 0.9	39.8 ± 2.0	-
calculated height (nm)	6.90 ± 0.24	14.45 ± 0.53	25.69 ± 1.15	40.64 ± 1.13	46.04 ± 4.46
average refractive index	1.394	1.380	1.367	1.353	1.350
monomer surface density (nm ⁻²)	42	62	87	86	55
monomer concentration in brush (nm ⁻³)	6.5	5.1	3.7	2.2	1.9
serum response (ng/cm ²)	14	14	10 (4)	28	44
serum resistance (compared to pure Au)	95%	95%	97% (99%)	91%	85%

^aFor 2 and 5 kDa, even higher concentrations than those specified can be used without reaching the cloud point. For 10 kDa, values in parentheses represent results for a hydroxyl-terminated polymer.

always assemble with an appropriate conformation and with sufficiently strong interactions, especially not on gold,⁶ which is often the material of choice for biosensors and bioelectronics. One option which can overcome all these limitations is “grafting-to” methods, where coils are grafted to the surface by forming a chemical bond, for instance, through a reactive end group on the polymer. The main problem with grafting-to is that unless the polymer is of quite low molecular weight¹⁷ the grafting densities become too low, since the binding to the surface is a reaction that tends to reach saturation when the coils start to overlap,¹⁸ which means that the dense brush regime is never reached. Instead, a less dense “mushroom” regime is often the result.¹⁹ This occurs when the distance between grafting points is comparable to the coil size in solution, i.e., when there is no significant overlap between neighboring coils. It is particularly challenging, or even considered impossible, to reach the “strongly stretched” regime where the brush height scales linearly with molecular weight.²⁰ Various grafting-to approaches for increased density have been suggested where polymers (quite often PEG) are grafted to the surface under conditions when the individual coils are shrunk, i.e., the free energy reduction the coils could gain from expanding (the excluded volume effect) is somehow suppressed. Shrinking of coils can be achieved by less favorable solvents²¹ or by conditions approaching those of a polymer melt^{22,23} (no solvent), both of which change the scaling law of coil size with molecular weight. However, existing grafting-to methods are often complicated to perform (e.g., temperature sensitive) or of limited use in practice. For instance, a solution approaching conditions of a polymer melt will be extremely viscous, which makes it impossible to use such an approach for functionalizing the interior of a small channel or a suspension of nanoparticles. It should also be noted that the mechanism of resistance to protein adsorption remains under debate, as several factors can contribute,^{2,24} such as conformational entropy of the coils and enthalpic contributions originating from hydrogen bonds in hydrated PEG.²⁵ Further, brushes are rarely characterized in terms of their height, even though this parameter clearly becomes important, e.g., in sensor applications.^{3,26} In addition, actual quantitative data of “biofouling” of PEG brushes prepared by grafting-to methods is scarce. Some studies do investigate protein adsorption, but then just for one²⁵ or a few^{12,23,27} proteins, and not an actual biological matrix. Finally, there is a lack of comparisons (within the same study) between the inertness of PEG brushes and the well-

known alkanethiol-based oligo(ethylene glycol) (OEG) self-assembled monolayers on gold,²⁸ which are commonly used for providing resistance to protein adsorption.^{6,27–29}

Here we present a new grafting-to method for PEG brushes which is based on a high salt concentration in water at room temperature, inspired by the “cloud point grafting” strategy.²¹ We use thiol-terminated PEG and graft them directly to gold, which is a widely encountered material in biointerface science. However, the concept is applicable also to other combinations of end groups and surfaces. We investigate the kinetics of the grafting process and the final brushes by surface plasmon resonance (SPR), quartz crystal microbalance with dissipation monitoring (QCM-D), and atomic force microscopy (AFM) for different molecular weights of PEG. The use of multiple techniques provides detailed information about the PEG brushes in terms of growth, grafting density, and thickness. This makes it possible for us to test if the brushes follow the de Gennes scaling law and if the height can be predicted using known parameters for atomic configuration and persistence length of PEG. Finally, we show quantitatively how the different brushes reduce the adsorption of proteins from complete (although 10× diluted) serum and discuss the relevant brush properties for achieving this goal.

EXPERIMENTAL SECTION

Chemicals. Methoxy-terminated PEG thiols (CH₃O-(CH₂CH₂O)_N-CH₂CH₂-SH, with *N* being the number of ethylene oxide units) had average molecular weights of 2000 (*N* ≈ 45), 5000 (*N* ≈ 113), 10 000 (*N* ≈ 227), 20 000 (*N* ≈ 455), and 30 000 Da (*N* ≈ 682) (Nanocs, New York, USA). The polydispersity index of all PEGs was between 1.02 and 1.08 with a purity of >95% according to the vendor. The hydroxyl-terminated 10 kDa PEG (RAPP Polymere, Tuebingen, Germany) had a polydispersity of 1.03 and purity >95%. The grafting solutions were prepared by dissolving and mixing the polymer in filtered (0.2 μm) solutions of 0.9 M Na₂SO₄ at room temperature (22 °C). In order to enhance binding rates, the concentration of PEG-SH was adjusted to be as high as possible without causing phase separation (aggregation) of the coils, i.e., just below the cloud point. (The concentrations used are summarized in Table 1.) For the QCM-D measurements, grafting was also tested in the following solutions: 0.6 M K₂SO₄ + 0.6 M NaCl at 22 or 50 °C, 3 M NaCl at 22 °C, and 0.15 M NaCl at 22 °C. The thiolated OEG (HO-(CH₂CH₂O)₆-(CH₂)₁₁-SH) (Prochimia, Gdansk, Poland), purity >95%, was dissolved in ethanol (99.7%) to a concentration of 1 mM and used within an hour of preparation. 10 mg/mL of bovine serum albumin (BSA) (Sigma-Aldrich) was dissolved in phosphate buffered saline (PBS) pH 7.4. Serum (bovine serum adult, Sigma-

Aldrich) was diluted in PBS to 10% by volume. Filtered (0.2 μm) aliquots of the BSA and serum solutions were used in the SPR experiments. The water used in this study was ASTM Research grade Type I ultrafiltered water (referred to as milli-Q water throughout the rest of this paper).

QCM-D. QCM-D measurements were performed on a Q-Sense E4 instrument (BioLin Scientific) equipped with a peristaltic pump (Ismatec). The gold sensor crystals were cleaned by immersion in RCA1 ($\text{H}_2\text{O}:\text{H}_2\text{O}_2$ (30%): NH_4OH (28–30%) = 5:1:1 v/v at 75 °C for 10 min) followed by rinsing with milli-Q water. The crystals were then sonicated in ethanol (99.7%) for 5 min and dried with N_2 . Prior to injections it was ensured that a stable baseline had been reached in the running buffer. Injections were allowed to reach saturation before rinsing with the running buffer. The measured frequency and dissipation shifts (third overtone) were taken as the difference before and after adsorption and rinsing. All experiments were performed at 22 °C unless stated otherwise.

SPR. SPR gold sensor slides with a gold thickness of ~ 50 nm were used for all SPR experiments (Bionavis, Ylöjärvi, Finland). Before usage each surface was cleaned according to the following protocol: 5 min of sonication in milli-Q water containing 2% cleaning agent (Hellmanex III, Hellma Analytics), rinsing with milli-Q water, RCA1 cleaning, sonication in ethanol (99.7%) for 5 min, and finally extensive rinsing with milli-Q water before drying with N_2 . Before inserting the sensor slide in the instrument, the backside was wiped with optical tissue wet with ethanol to remove any dust. All SPR experiments were performed at 22 °C in a SPR Navi 220A instrument (BioNavis). The instrument was equipped with a flow cell containing two separate channels which can operate in either parallel or serial mode. The laser wavelength used for the measurements was 670 nm with the exception of the wet thickness determinations, where a wavelength of 785 nm was used.

Binding of PEG and OEG. First, a blank spectrum of the gold sensor was recorded in air. Afterward the flow cell was filled and rinsed with milli-Q water until the baseline stabilized. The milli-Q water was then exchanged to Na_2SO_4 in one of the flow channels and the flow rate was set to 15 $\mu\text{L}/\text{min}$, and at least 30 min passed before the polymer solution was injected. Once the injection had reached a plateau the channel was rinsed with Na_2SO_4 to get the final shift and the solvent was then exchanged back to milli-Q water. To prepare the second flow channel, to be used as a reference for the height measurements, grafting of OEG was conducted with ethanol (99.7%) as the running buffer. The OEG solution was injected for at least 45 min at 10 $\mu\text{L}/\text{min}$ followed by rinsing with ethanol and then exchanging the solution back to milli-Q water. The sensor slide was then dried with N_2 and the spectra of the surface with the grafted polymer was recorded in air.

Dry Thickness Determination. Before and after binding the PEG the angular spectrum was recorded in air. The spectra were then fitted to standard Fresnel models.³⁰ First, the reflectivity of only the finite metal film was fitted allowing the complex permittivity and thickness to vary. Other parameters (wavelength and refractive index of prism) were set to their specified values. After establishing the parameters describing the metal films (including the Cr adhesion layer) and verifying that they were reasonable, the same values were used when fitting the reflectivity spectrum after PEG grafting, but with an additional dielectric film with the refractive index of dry PEG¹¹ (1.456). In separate experiments we also determined the refractivity of PEG (Supporting Information) to 0.134 cm^3/g , in good agreement with the literature,³¹ which was then used to calculate the average refractive index values for the brushes. The values are summarized in Table 1.

BSA Method (Brush Height Determination). First, the running buffer was exchanged for PBS in both channels. In serial mode four consecutive injections were made at a flow rate of 40 $\mu\text{L}/\text{min}$ for 5 min, with a 5 min rinse with the running buffer in between each injection. The shift in angle for each injection was taken as the end value of the injection minus the baseline after 4 min of rinsing with PBS. A step-like profile (bulk response) upon injections was verified before using data to calculate brush height.

Serum Tests. Serum resistance was measured by injecting the diluted serum solution for 50 min at a flow rate of 5 $\mu\text{L}/\text{min}$ and rinsing with PBS. The shift in angle was taken as the difference between the PBS baseline after and prior to the injection. The serum response was quantified using a bulk sensitivity of 121 deg per RI unit, a field decay length of 218 nm calculated in water for a surface plasmon of vacuum wavelength 670 nm³² (equation used and its derivation in Supporting Information), and an average value of 0.184 cm^3/g for protein refractivity.^{33,34}

AFM. Gold coated glass slides were cleaned by immersing them for 10 min in RCA1 followed by 30 min immersion in water. The slides were then sonicated in ethanol for 15 min, dried in a N_2 stream, and incubated overnight with SH-PEG in 0.9 M Na_2SO_4 while stirring at room temperature. After rinsing with milli-Q water, the samples were dried in a nitrogen gas stream and mounted on a sample holder. A Bioscope catalyst AFM (Bruker, U.S.) with gold coated OBL-10 cantilevers (Bruker, U.S.) with spring constant 0.006–0.009 N/m was used to record force volume maps of the modified substrate. Before use, the cantilevers were passivated using droplet incubation of 1 mM $\text{C}_{17}\text{H}_{36}\text{O}_4\text{S}$ (nanoScience Instruments, USA) in PBS for 10 min and rinsed with PBS. Each 500 \times 500 nm^2 force volume map was recorded with 32 \times 32 data points or 1024 force curves in PBS. The ramp size was 500 nm and the maximum (trigger) force applied was 500 pN. After the measurement additional force curves were obtained on a clean glass substrate in PBS as a control for tip contamination. Baseline corrected force–distance curves were fitted with an exponential curve using an Igor script (WaveMetrics). The contact point was obtained by setting a force threshold of 1 pN for the fit to the experimental data. Higher threshold (5 pN) gave lower ($\sim 20\%$) brush heights as expected since the tip pushes the PEG down to a high extent before reaching the contact force.

RESULTS AND DISCUSSION

Quartz Crystal Microbalance. As a first step we evaluated how much PEG-SH could be grafted to Au under different conditions in terms of temperature and concentration of different salts, using QCM-D for simplicity and high throughput. The response from complete serum adsorption (after changing to PBS as solvent) was also measured for the different PEG coatings and for pure gold. Results are summarized in Figure 1, which shows saturated shifts in frequency and dissipation, in this case for 5 kDa PEG-SH. All binding reactions were allowed to reach saturation and no reversible binding was observed for PEG or serum, i.e., there was no signal upon rinsing.

As can be seen in Figure 1, the response from the polymer generally increases at higher ionic strength (for the salts NaCl , K_2SO_4 , and Na_2SO_4) during grafting with the lowest signal for the case of only 150 mM NaCl . The highest QCM-D frequency response from PEG is achieved when grafting in 0.9 M Na_2SO_4 , indicating that this situation provides the highest grafting density. The pure gold surface gives a high response from exposure to serum as expected, while the protein binding becomes comparable to the noise level in QCM-D for all PEG coatings. The only exception is PEG grafted in 150 mM NaCl , which probably does not provide high enough grafting density for significant coil stretching and brush formation. The increased grafting density at higher salt concentrations can be understood as due to an osmotic balance, considering PEG as a sponge which takes up a lot of water and swells, while under conditions of high ionic strength water is extracted from the coil, thereby shrinking it so that more coils can fit on the surface. The reason 0.9 M Na_2SO_4 gives the highest grafting density is likely that SO_4^{2-} is a strongly hydrated ion that can “salt out” the PEG efficiently.³⁵ The mixture of K_2SO_4 and NaCl (0.6 M each) did not provide higher grafting density,

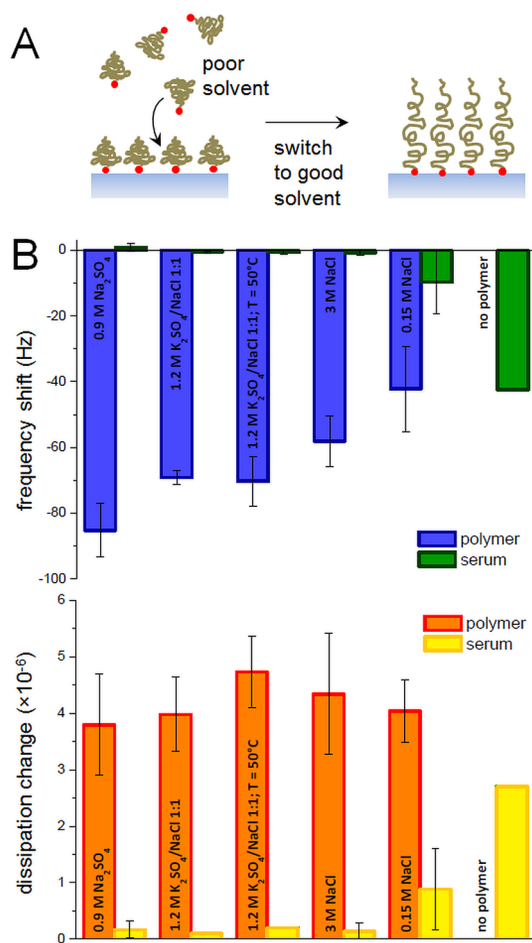


Figure 1. Grafting of 5 kDa thiolated poly(ethylene glycol) using increased salt concentration or elevated temperatures to achieve higher grafting densities. Part (A) illustrates the principle of “close to cloud point grafting”. Part (B) shows saturated quartz crystal microbalance signals (frequency and dissipation) and the response from serum.

suggesting divalent anions are more important for the grafting compared with monovalent anions. Heating the solution to 50 °C did not have any strong influence on the grafting density either. Early studies of the effect of salts on the solubility of PEG in solution showed dependence on the concentration used and valency of the ions.³⁵ A similar behavior to the Hofmeister series, describing the salting out effect of various salts on proteins, was observed for the effectiveness of salting out PEG. These findings were attributed to the effectiveness of disrupting the water bound to the ether oxygens of the polymer.^{35,36} Other studies have shown that the effect of the anion is dominant in lowering the cloud point for PEG.^{37,38} In one of the studies the cloud point mechanism was explained by a salt-deficient zone close to the polymer due to repulsive ion–polymer interactions.³⁸ This model, based on interference with the hydration shell of polymers, has also more recently been used to describe some parts of the clouding behavior for a thermoresponsive polymer.³⁹ However, the efficiency of salting out never follows generic trends and always varies depending on the combination of polymer and salt used.⁴⁰ (To our knowledge these effects are still not fully understood.)

We also attempted to analyze the QCM-D results to determine the brush thickness by multiple parameter viscoelastic models using data from different overtones.^{41,42}

However, this analysis requires assuming a coupled water content for the brush, which is not necessarily equal to the full water content. This is a parameter which can only be acquired by educated guessing and thus we choose not to include any detailed analysis of QCM-D data for brush height determination in this study. (Depending on the degree of hydration the estimated heights for the 5 kDa brushes in Na₂SO₄ and K₂SO₄ + NaCl lie somewhere between 10 and 20 nm.) Finally, although good inert properties are suggested by the data in Figure 1B, QCM-D is not the ideal method to quantify the amount of adsorbed serum proteins because it does not have the lowest detection limit (e.g., compared with SPR). Further, it is always challenging to accurately account for the water contribution to the signal⁴² since there may be proteins adsorbing to the sensor crystals which to some extent replace coupled water, making their contribution to the response lower. Hence we consider SPR more reliable for quantifying protein adsorption (see below). Optical techniques also have the advantage of responding linearly with the protein coverage.²⁶

Surface Plasmon Resonance. Following the results from QCM-D, the grafting of PEG-SH in 0.9 M Na₂SO₄ was studied for molecular weights of 2, 5, 10, 20, and 30 kDa. We used different so-called critical concentrations, above which the PEG phase separates in 0.9 M Na₂SO₄ at room temperature, for the different molecular weights as summarized in Table 1. If the cloud point was actually surpassed so that the PEG phase separated from the ionic solution (visible by eye) the grafting did not produce dense resistant brushes. This could be due to inefficient mass transport of PEG aggregates to the surface and poor accessibility of the thiol group in the collapsed globule. One could thus refer to our method as “close-to-cloud-point grafting”. The critical concentrations are more than 1 order of magnitude below the values where one can expect *overlapping* of coils in solution. (Using the cube of the Flory radius as a high estimate of coil volume, the concentrations used when grafting were all at least 1 order of magnitude lower than that corresponding to one coil per R_F^3 .) We also verified that the binding of PEG-SH was specific by testing PEG without a thiol group, which did not yield any detectable binding to gold.

In order to quantify the grafting density full angular scan reflectivity spectra were measured by SPR in air (dry films). As illustrated in Figure 2A for 20 kDa before and after PEG grafting, binding shifts the resonance to a higher angle. The reflectivity spectra were then fitted to standard Fresnel models to determine the thickness of the dry polymer layer. In this step the literature value for refractive index of dry PEG¹¹ (1.456) was used (which was the only parameter allowed to vary). The full spectra were well described by the models as exemplified in Figure 2A. Next, after determining the thickness of the dry films, the bulk density of PEG (1.09 g/cm³) was used to calculate the grafting density through the known molecular weights. The calculated grafting densities are shown in Figure 2B and summarized in Table 1.

SPR measurements were also used to monitor the grafting in 0.9 M Na₂SO₄ in real time as shown in Figure 2C. Binding kinetics are presented for all different molecular weights investigated. For 2, 5, and 10 kDa PEG-SH the binding is relatively fast, while it becomes much slower for 20 kDa and 30 kDa. The SPR instrument is designed to measure binding under constant flow with an efficient delivery of molecules in order to prevent influence from mass transport. With the flow rate used (15 μ L/min) the Peclet number is much larger than unity, suggesting a thin depletion zone compared to the height

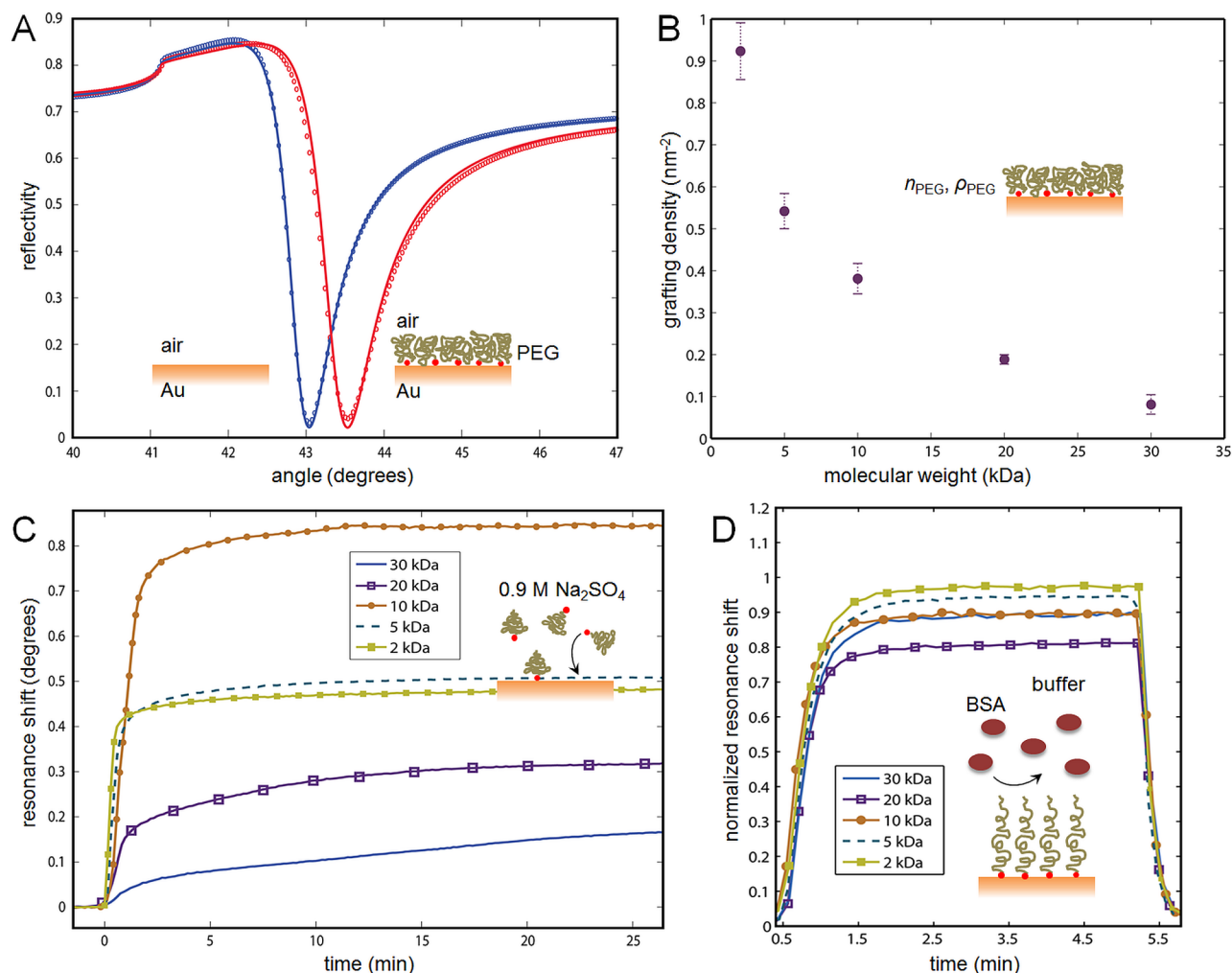


Figure 2. SPR measurements on grafting in Na₂SO₄ and the resulting brush properties. Part (A) shows an example of the full angular spectrum of a clean gold surface and a surface modified with a 20 kDa brush in air. The lines show Fresnel fits to the experimental spectra. Part (B) shows the calculated grafting densities for the different molecular weights, treating the dry coating as bulk poly(ethylene glycol). Part (C) shows binding kinetics for different molecular weights (polymer introduced at time zero, concentrations given in Table 1). Part (D) shows the responses to injections of bovine serum albumin, which is used as a noninvasive probe for determining the brush height.

of the channel⁴³ (Supporting Information). We thus believe that any influence from mass transport is negligible, in agreement with the “Langmuir shape” of the binding curves. The different binding rates are naturally to some extent due to the fact that higher concentrations were used for smaller PEGs (Table 1). Still, the binding of the larger PEGs is *very* slow (saturation required ~ 5 h for 20 kDa and 30 kDa) even though the change in concentration was less than an order of magnitude compared to binding of 10 kDa PEG-SH, which exhibited fast saturation (~ 10 min). Reduced binding must occur sooner or later for sufficiently large coils since the entropy loss upon grafting increases with coil size.¹⁸ The slow binding may be related to the accessibility of the terminal group, which should decrease with molecular weight following a surface to volume scaling argument. With this we mean that the probability that the terminal group is close to the “surface” of the coil must be smaller if the coil occupies a larger volume. (Considering a polymer which is so small that the contour length is comparable to the persistence length, the end group is always accessible.) Another plausible explanation is that the already grafted coils form a barrier for further grafting and that this barrier increases with molecular weight. However, it should

be kept in mind that the enthalpic contribution of grafting, i.e., bond formation, is different for other combinations of surfaces and reactive groups. This could mean that even higher grafting densities can be reached in 0.9 M Na₂SO₄ by using another type of coupling chemistry. The Au–S bond is only semicovalent, with a strength of $\sim 84 k_B T$ at room temperature.⁴⁴ The exact binding enthalpy naturally depends on the type of thiol⁴⁵ but always lies much below a typical covalent bond strength.

In order to determine the heights of the PEG brushes, we use the recently presented SPR method based on changes in the refractive index of the bulk liquid by “non-invasive probes”.^{46,47} As in previous use of this method, we injected bovine serum albumin (BSA) as a probe and compared the response with an OEG monolayer reference surface. We carefully determined a single field decay of 368 nm (when measuring at 785 nm) to use in the calculations (Supporting Information). Note that this is an effective field decay which takes into account that the decay is higher in the PEG brush due to its higher refractive index, which enters as a parameter in the iterative process.⁴⁷ Figure 2D shows the SPR response to BSA injections normalized to the reference channel. As expected, the

normalized response is lower for PEG brushes of higher molecular weight until the trend is changed for the case of 30 kDa. Note that one condition for the height determinations to be accurate is that the response from the probe is fully reversible in both channels, which is the case for the data in Figure 2D, proving that there was no irreversible adsorption of BSA to Au. In general, acquiring both thickness and RI for a film is challenging when using SPR since the parameters are intimately connected.²⁶ (Typically, the same response is achieved as long as the product of refractive index change and thickness is constant.) Even in ellipsometry it is not straightforward to accurately model the reflectivity of all interfaces and both thickness and refractive index appear as coupled parameters in the models. Various methods have been suggested to overcome this limitation, such as dual-wavelength SPR measurements.⁴⁸ However, that method requires several unknown parameters and is based on utilizing the very small change of RI with wavelength (dispersion) for the thin film. For all these methods one must also make the assumption that the film has homogeneous density along the direction perpendicular to the surface, which is not the case for polymer brushes.⁷ In contrast, the method of noninvasive probes requires only the decay length of the evanescent field and the thickness of an inert film in a reference channel. Another advantage for the method used is that the thickness is acquired directly rather than being calculated through another parameter such as the grafting density. Importantly, not even the refractive index of the film is needed. Brush heights are summarized in Figure 4 and Table 1.

Atomic Force Microscopy. In order to further verify the brush height we performed liquid phase AFM scans on the PEG brushes. As shown earlier,^{47,49} one can push the AFM tip through the brush until it reaches the solid surface, and using a threshold force one can extrapolate the contact height of the brush. This can lead to an underestimate of brush height if the threshold force is set too high⁴⁹ and thus we used a low threshold value which was still distinguishable from the noise⁴⁷ (1 pN). Figure 3 shows histograms of brush height for the PEG sizes of 5, 10, and 20 kDa and a comparison with other height determinations is given in Figure 4.

Comparison with Theory. In order to calculate the expected height H of the PEG brushes by theory we use the following model (derived in Supporting Information):

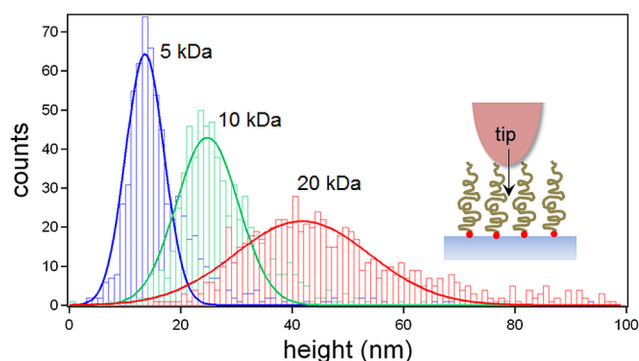


Figure 3. Atomic force microscopy histogram of measurements of brush heights for three sizes of poly(ethylene glycol) grafted in 0.9 M Na_2SO_4 . The tip is pushed through the brush until it contacts the hard surface.

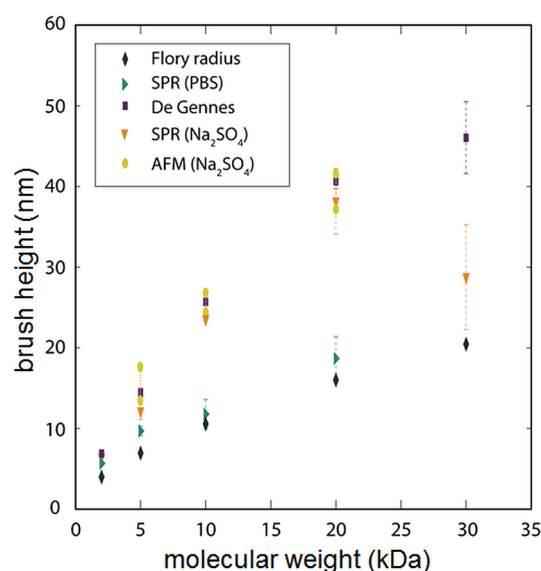


Figure 4. Summary of brush heights determined by surface plasmon resonance (triangles pointing down), by eq 1 (squares) and by atomic force microscopy (circles). For comparison, the heights of poly(ethylene glycol) grafted without Na_2SO_4 are also shown (triangles pointing right) together with the Flory radius (diamonds).

$$H = \left[\frac{\Gamma}{3} \right]^{1/3} b^{2/3} a N \quad (1)$$

Here Γ is the grafting density (nm^{-2}), a is the chemical monomer length (nm), b is the Kuhn length, i.e., twice the persistence length (nm), and N is the degree of polymerization, i.e., the number of chemical monomers (defined from the molecular weight M). It is clear that the power laws in eq 1 for Γ and N are identical to those first identified by de Gennes.²⁰ When calculating the heights of the brushes one must choose carefully the values for both molecular contour length (aN) and Kuhn length (b). For PEG in water at room temperature, literature values of the Kuhn length are quite similar. Examples are $b = 0.76 \text{ nm}$ ⁵⁰ and $b = 0.7 \text{ nm}$ ³⁶ measured by AFM on single molecules or $b = 0.74 \text{ nm}$ from molecular dynamics simulations of short chains.⁵¹ (We used $b = 0.72 \text{ nm}$.) The monomer ($\text{CH}_2\text{CH}_2\text{O}$) forms a quite compact structure in water known as trans–trans–gauche³⁶ or helical conformation⁵² due to hydrogen bonding. There is consensus that the monomer size is $a = 0.28 \text{ nm}$ in water (like in the crystalline state).^{36,52} Note that we are not claiming that our values of a and b are representative of PEG in 0.9 M Na_2SO_4 , but they should be valid for calculating the height of the brush once it is in PBS.

It seems likely that the reason such high grafting densities (Figure 2B) can be reached in 0.9 M Na_2SO_4 is that it acts as a theta solvent. In a theta solvent the scaling of characteristic polymer size with molecular weight is closer to $M^{1/2}$, rather than $M^{3/5}$. This means that the factor by which the coils shrink when Na_2SO_4 is introduced would increase with M , which leads to the prediction that higher molecular weights should give a more pronounced effect for our grafting strategy (compared to grafting in water) when looking at brush thickness. Comparable values for the grafting density in this study have only been achieved on highly curved surfaces that relax the entropy loss by offering a larger expansion volume per coil.⁵³ The most significant source of error when calculating grafting density here

is likely that the density and refractive index of a thin dry PEG film could differ somewhat from that of bulk PEG. However, the grafting density should only have a weak influence on the brush height (see eq 1).

All results on brush thickness, experimental and theoretical, are summarized in Figure 4. The heights measured directly by SPR are shown (triangles) together with the calculated heights (squares). The error bars for the calculated heights are due to variations in the experimental values for grafting density, which must be inserted in eq 1 when calculating the height. Clearly, the experimental SPR values are very close ($\sim 10\%$ lower) to the calculated heights. Further, this offset is approximately the same for all sizes of PEG, showing that the brushes follow the de Gennes scaling law even though they are prepared by a grafting-to method. It should be kept in mind that according to eq 1 the plot in Figure 4 should be fully linear because the same grafting density is not maintained as M is increased. The only clear deviation from theory is observed for 30 kDa, which has an experimental value more than 30% lower than the calculated height. This is likely because the grafting density is simply too low for the brush to reach the strongly stretched regime, in agreement with the weaker binding observed in SPR (Figure 2C). This suggests that our method no longer provides thick and dense brushes for PEGs of 30 kDa or more, at least not for the case of thiol-gold coupling. Figure 4 also shows the average AFM heights, in good agreement with the other values. We further compare our brush heights with those obtained by grafting under “ordinary” conditions, i.e., simply letting the PEG-SH react with gold in aqueous PBS buffer.^{47,49} The PEG concentrations used then were typically 1–2 orders of magnitude higher (1 mM). Regardless, especially for higher molecular weights it is clear that grafting in 0.9 M Na_2SO_4 results in a much higher thickness and a scaling law that is closer to M instead of $M^{3/5}$. Also, the absolute heights of the other coatings (which are mushrooms and not brushes) are in good agreement with the Flory radius of a coil in solution (also plotted), which shows that there is no significant coil overlap on the surface and hence no significant extension.

Strictly speaking, one should be careful when using terms as “brush height” since it is quite unphysical that the monomer concentration would follow a step function when moving closer to the surface. There must, at least to some extent, be a *gradual* increase in monomer concentration. Using the measured grafting density and height we can generate the density profile for the brushes assuming a parabolic model based on self-consistent field theory⁷ (Figure 5). This model differs from the step function model (eq 1) which treats the coils as a homogeneous “gas” of monomers (the Flory argument). The “maximum height” (where the monomer density becomes zero) for a brush in the parabolic density model is 1.3 times the height estimated by eq 1.⁷ By also using the condition that the total number of monomers per area remains the same, the plot of monomer concentration against distance from the surface can be generated (further explained in Supporting Information). Here we exclude the results for 30 kDa since those brushes did not follow the theory well. Assuming the theoretical monomer density profiles in Figure 5 are accurate, it is interesting to think of how this influences the height determinations with BSA. It seems plausible that the protein actually penetrates the very top region of the parabolic brush where the monomer density is sufficiently low and this might be the reason why eq 1, which defines the “height” as 77% of the height of the furthest extended monomers, provides good

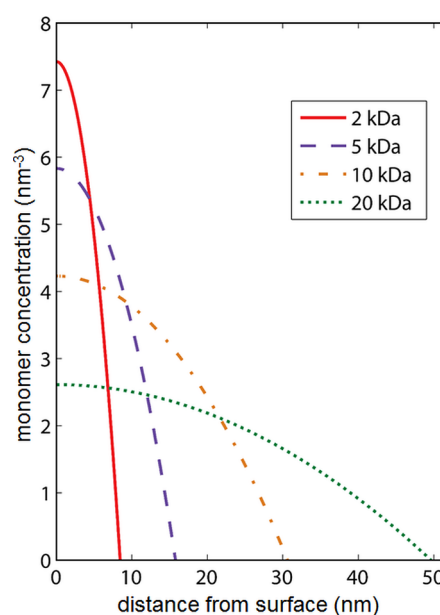


Figure 5. Monomer concentration as a function of distance from the surface according to the parabolic density profile model. The experimentally determined values of grafting density and brush height were used to generate the plots.

agreement with experiments. The density profiles are also in good agreement with the AFM histograms of brush contact height in Figure 3.

Protein Resistance. After characterizing the PEG brushes, we investigated their inertness toward biomolecular adsorption using SPR. Here we also included a self-assembled monolayer of the oligo(ethylene glycol) with 6 EG units and $-\text{OH}$ termination, as well as a 10 kDa PEG with $-\text{OH}$ termination for comparison. Results are summarized in Figure 6, including the response from an unmodified gold surface, all exposed to $10\times$ diluted serum in buffer for 50 min. It should be noted that the data in Figure 6B represents irreversible binding, i.e., serum proteins that induce an SPR signal, which remains after rinsing with buffer (example in Figure 6A). Although some reversible binding cannot be excluded in the SPR response, proteins are generally expected to adsorb irreversibly on gold and the QCM-D data showed no signs of reversible binding, i.e., no change upon rinsing. The SPR response from a serum injection is thus mainly attributed to the high bulk RI of the serum solution. It is clear that the 2, 5, and 10 kDa brushes provide good serum resistance and outperform the OEG monolayer. The best performance is achieved for $-\text{OH}$ terminated 10 kDa ($\sim 99\%$ resistance), which corresponds to an amount of adsorbed proteins of $4 \text{ ng}/\text{cm}^2$. The coverage on pure gold was calculated to be $297 \text{ ng}/\text{cm}^2$. Here the thickness of the adsorbed serum layer does not influence the result significantly as long as it is well below the decay length of the evanescent field (see Supporting Information). Even though the $-\text{OH}$ terminated 10 kDa PEG performs better than the $-\text{CH}_3$ terminated the effect is small and further investigations are suggested to conclude if this is truly an effect of the terminal group, especially since studies on OEG monolayers have not observed this effect.²⁷ The 20 kDa performs similarly to the OEG, while for 30 kDa poorer inertness is observed. Also, a trend of increased protein repellent properties with brush height can be seen, but it stops at 20 kDa. It is probably no coincidence that between 10 and 20

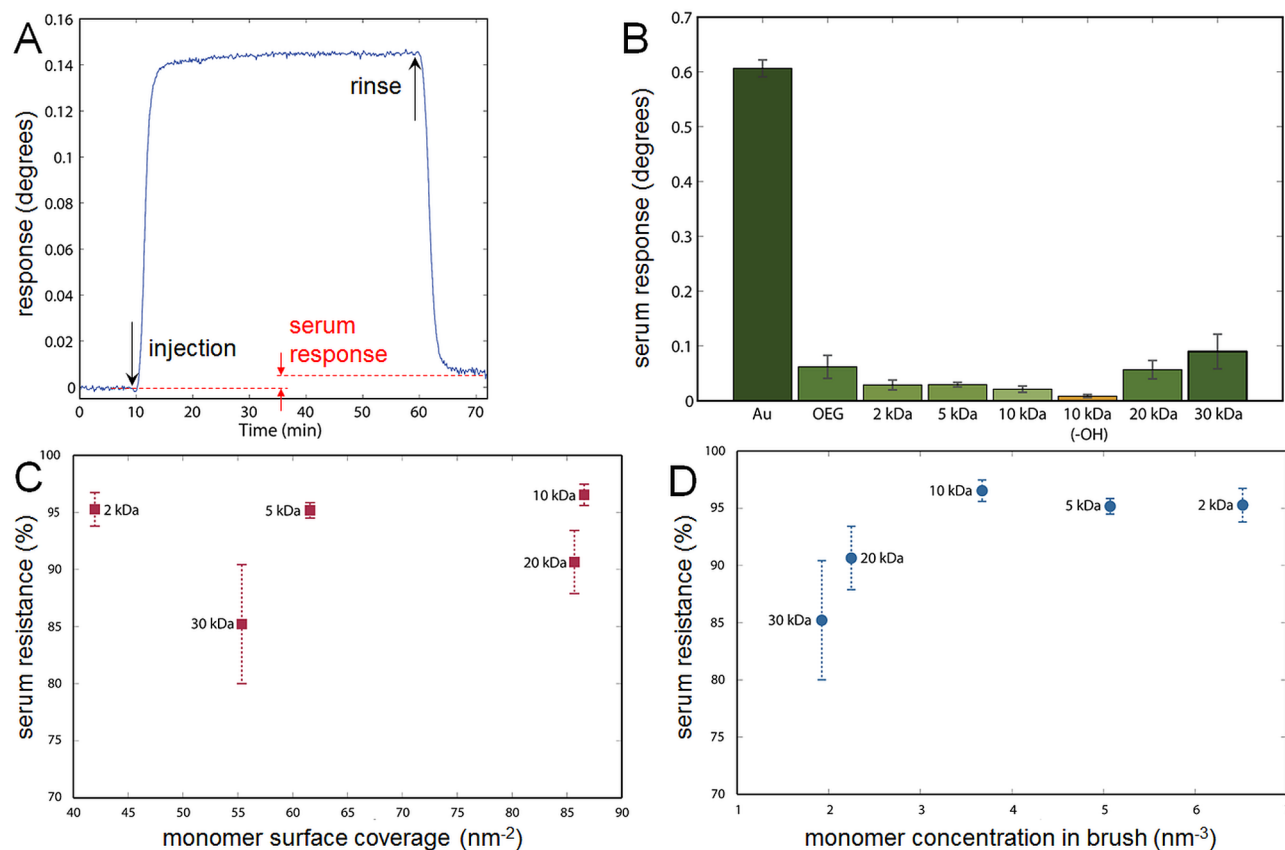


Figure 6. Serum protein adsorption on poly(ethylene glycol) brushes on gold measured with surface plasmon resonance. Results from oligo(ethylene glycol) monolayers are included for comparison. Part (A) shows a typical serum injection and illustrates the total response, defined as the shift after 50 min exposure. (Most of the immediate signal is due to the high refractive index of the serum solution.) Part (B) shows the final signals, part (C) the serum resistance (fraction reduced response compared to pure gold) vs monomer surface coverage, and part (D) serum resistance vs average monomer concentration inside the brush.

kDa also the binding kinetics of grafting start to become quite slow (Figure 2C).

Comparing the protein repellent properties presented in this study with earlier literature indicates that we are able to reach about the same values as those reported for PLL-*g*-PEG.^{12,54} In those studies the interface was exposed to nondiluted serum which might indicate that their repellent properties are even greater. However, even with 10× dilution (in part to prevent clogging of the fluidic systems) the protein concentration is very high (~10 g/L). Also, PLL-*g*-PEG binds to surfaces which are negatively charged (e.g., Nb₂O₅, TiO₂, and SiO₂) and is not applicable to functionalization of gold. One can also compare our results to a previously tried cloud point strategy with PEG to gold using 1 M NaCl at 37 °C.⁵⁵ For a 5 kDa brush, adsorption resistance (fraction reduced response compared to pure gold) toward a cell culture medium was then 77%, and with a combination of 2 and 5 kDa, a maximum resistance of 93% was reached.⁵⁵ As another comparison, a cloud point strategy utilizing a combination of salt and temperature provided adsorption resistance of 70–90% upon exposure to lysozyme and fibrinogen.^{56,57}

When comparing protein resistance one important point is that the protein repellent properties could be different depending on the *time scale* of the experiment; i.e., the brushes may be kinetic energy barriers rather than equilibrium constraints. Based on theoretical models it has been suggested that PEG brushes larger than ~2 kDa are essentially kinetic

barriers.⁵⁸ The absorbed amount of protein might therefore be increased for longer or repeated exposure. We tested this by repeated injections of complete serum over a long time and could detect a weak but barely significant trend of increasing protein adsorption with number of injections (Supporting Information). However, it is clear the PEG brushes are highly inert on the time scale of a typical experiment (hours, up to at least 1 day) and suitable for use in, e.g., surface-based biosensors³ or for patterning by material-selective functionalization.⁶ (For very long-term applications such as implants, PEG is in no way suitable due to oxidative instability.)

Since we have determined both grafting density and thickness for the brushes, we can also plot resistance toward serum protein adsorption against specific brush parameters. Figure 6C shows a plot of resistance vs monomer surface density, which gives no clear correlation. One usually refers to a value of ~20 monomers per nm² as a requisite for protein resistance.⁵ All brushes are well above this limit, which could be the reason there is no correlation in Figure 6C. We can also make a plot of serum resistance against monomer *concentration* inside the brush (Figure 6D). Here it should be kept in mind that the monomer concentration varies with distance from the surface⁷ (Figure 5) so these values represent an average. Still, the plot in Figure 6D shows that the monomer concentration decreases monotonically with PEG molecular weight and suggests a trend in that higher monomer concentration seems to improve resistance to adsorption. This relates back to the

theory that these brushes provide a kinetic rather than an equilibrium barrier toward protein adsorption.⁵⁸ The free energy barrier for a protein that enters the brush should increase with monomer concentration. However, the physical thickness of this steric barrier should also come into play, and tentatively, the reason 10 kDa performs best is that it represents a good trade-off between monomer concentration and thickness. Under the assumption that the parabolic profiles (Figure 5) are accurate this kind of detailed information on brush morphology should in the long run contribute to a better understanding of adsorption resistance.

One can speculate on the reason a small amount of protein adsorption does occur despite the PEG brushes and how one could improve protein resistance even further. One possible explanation for adsorption is defects or impurities on the surface. For instance, a nonplanar surface with nanoscale curvature could influence the brush morphology^{5,49,59} which might lead to poorer repelling properties. Also, any contamination on the surface will likely prevent proper grafting, so perhaps the response from serum could be reduced further by extreme carefulness and further optimization when it comes to cleaning and handling the surfaces. However, this should not be required if the method is to be simple to apply for a great variety of users in biointerface science. One previously suggested method for improving the nonfouling properties further is “backfilling” of exposed or defect regions,²⁹ i.e., to graft a smaller PEG (or even OEG) after the binding of the initial layer. We tested this approach in QCM-D and SPR but in all cases we observed a *negative* response when introducing the smaller PEG, even in ordinary buffer. The only reasonable interpretation we can think of for such behavior is that the smaller PEG replaces the larger one. For polystyrene brushes it has been suggested that it is possible for any free coil to penetrate the brush when the radius of gyration is smaller than that of the grafted coils⁴¹ and replacement processes have been observed for alkanethiols on gold.⁶⁰ From an equilibrium perspective this is not surprising considering that the entropy loss upon grafting must increase with polymer size and that more thiol-gold bonds can be formed for the case of smaller thiolated molecules. On the other hand, considering the kinetic aspects of such a replacement process, it is surprising that the underlying gold surface is so easily accessible for the smaller PEG-SH. We find it quite surprising that the results suggest that a 10 kDa brush is almost fully resistant to serum but fails entirely to prevent adsorption (and is even “kicked out”) by another thiol-PEG that has a lower molecular weight.

CONCLUSIONS

In summary, we have presented a grafting-to method that provides strongly stretched brushes of PEG. Besides this scientifically interesting result, we have also shown important technological implications through the good inert properties of the brushes. First of all, the method is extremely simple since it is just based on dissolving the PEG in 0.9 M Na₂SO₄ at suitable concentrations (Table 1). There is no need to increase temperature and any kind of surface in contact with water can be modified because the grafting solution flows easily. We emphasize that the brushes have been exposed to complete serum (although diluted 10×) for 50 min and not just a few proteins. If one wants to prepare a functionalized surface (not just one that is inert) this is straightforward because one can simply use PEGs with suitable terminal groups (for instance, –COOH groups linking to –NH₂ groups in subsequent steps).

We have characterized the PEG brushes with multiple techniques and determined both grafting density and thickness. Knowing the thickness of the resulting brush is especially useful when functionalizing surfaces for biomolecular detection because the distance from the surface determines the response of, for instance, optical label-free biosensors.^{3,26} In combination with the known narrow molecular weight distributions, the brushes are thus quite well-characterized. This makes it possible to acquire more information about which properties are essential for resistance to biomolecular adsorption. We have analyzed the influence from both monomer surface coverage and monomer concentration inside the brush. Monomer surface coverage appears irrelevant in our range (40–90 EG/nm²). It seems plausible that the brushes are mainly kinetic barriers and that a thick region (~10 nm) with high monomer concentration (~4 EG/nm³) is needed to provide good resistance to adsorption (>95%).

For future work, we are interested in using the grafting-to method on plasmonic nanostructures.³ This may improve the specificity in biomolecular detection but can also be used to experimentally address fundamental questions about the behavior of polymers on curved interfaces, a topic which has so far mainly been addressed by theory.⁵⁹

ASSOCIATED CONTENT

Supporting Information

Theoretical derivation of the expected polymer brush height. Theory, extra data, and further details on SPR. Discussion on influence from mass transport on binding kinetics. This material is available free of charge via the Internet at <http://pubs.acs.org>.

AUTHOR INFORMATION

Corresponding Author

*E-mail: adahlin@chalmers.se.

Present Address

#Laurent Feuz, Hedwigstrasse 12, 8032 Zurich, Switzerland.

Author Contributions

The manuscript was written through contributions of all authors. All authors have given approval to the final version of the manuscript.

Notes

The authors declare no competing financial interest.

ACKNOWLEDGMENTS

This work was sponsored by the Swedish Research Council, the Swedish Foundation for Strategic Research, and the EU FP7Marie Curie Action.

ABBREVIATIONS

PEG, poly(ethylene glycol); OEG, oligo(ethylene glycol); SPR, surface plasmon resonance; QCM-D, quartz crystal microbalance with dissipation monitoring; AFM, atomic force microscopy; BSA, bovine serum albumin

REFERENCES

- (1) Hucknall, A.; Rangarajan, S.; Chilkoti, A. In pursuit of zero: Polymer brushes that resist the adsorption of proteins. *Adv. Mater.* **2009**, *21*, 2441–2446.
- (2) Schlenoff, J. B. Zwitteration: Coating surfaces with zwitterionic functionality to reduce nonspecific adsorption. *Langmuir* **2014**, *30*, 9625–9636.

- (3) Mazzotta, F.; Johnson, T. W.; Dahlin, A. B.; Shaver, J.; Oh, S.-H.; Hook, F. Influence of the evanescent field decay length on the sensitivity of plasmonic nanodisks and nanoholes. *ACS Photonics* **2015**, *2*, 256–262.
- (4) Vaisocherova, H.; Yang, W.; Zhang, Z.; Cao, Z. Q.; Cheng, G.; Piliarik, M.; Homola, J.; Jiang, S. Y. Ultralow fouling and functionalizable surface chemistry based on a zwitterionic polymer enabling sensitive and specific protein detection in undiluted blood plasma. *Anal. Chem.* **2008**, *80*, 7894–7901.
- (5) Amstad, E.; Textor, M.; Reimhult, E. Stabilization and functionalization of iron oxide nanoparticles for biomedical applications. *Nanoscale* **2011**, *3*, 2819–2843.
- (6) Marie, R.; Dahlin, A. B.; Tegenfeldt, J. O.; Hook, F. Generic surface modification strategy for sensing applications based on Au/SiO₂ nanostructures. *Biointerphases* **2007**, *2*, 49–55.
- (7) Milner, S. T. Polymer brushes. *Science* **1991**, *251*, 905–914.
- (8) Bolduc, O. R.; Clouthier, C. M.; Pelletier, J. N.; Masson, J. F. Peptide self-assembled monolayers for label-free and unamplified surface plasmon resonance biosensing in crude cell lysate. *Anal. Chem.* **2009**, *81*, 6779–6788.
- (9) Holmlin, R. E.; Chen, X. X.; Chapman, R. G.; Takayama, S.; Whitesides, G. M. Zwitterionic SAMs that resist nonspecific adsorption of protein from aqueous buffer. *Langmuir* **2001**, *17*, 2841–2850.
- (10) Statz, A. R.; Meagher, R. J.; Barron, A. E.; Messersmith, P. B. New peptidomimetic polymers for antifouling surfaces. *J. Am. Chem. Soc.* **2005**, *127*, 7972–7973.
- (11) Mark, J. E. *Polymer data handbook*; Oxford University Press: New York, 1999; p xi, 1018 p.
- (12) Kenausis, G. L.; Voros, J.; Elbert, D. L.; Huang, N. P.; Hofer, R.; Ruiz-Taylor, L.; Textor, M.; Hubbell, J. A.; Spencer, N. D. Poly(L-lysine)-g-poly(ethylene glycol) layers on metal oxide surfaces: Attachment mechanism and effects of polymer architecture on resistance to protein adsorption. *J. Phys. Chem. B* **2000**, *104*, 3298–3309.
- (13) Ma, H. W.; Hyun, J. H.; Stiller, P.; Chilkoti, A. "Non-fouling" oligo(ethylene glycol)-functionalized polymer brushes synthesized by surface-initiated atom transfer radical polymerization. *Adv. Mater.* **2004**, *16*, 338–341.
- (14) Huang, N. P.; Michel, R.; Voros, J.; Textor, M.; Hofer, R.; Rossi, A.; Elbert, D. L.; Hubbell, J. A.; Spencer, N. D. Poly(L-lysine)-g-poly(ethylene glycol) layers on metal oxide surfaces: Surface-analytical characterization and resistance to serum and fibrinogen adsorption. *Langmuir* **2001**, *17*, 489–498.
- (15) Malmsten, M.; Linse, P.; Cosgrove, T. Adsorption of PEO-PPO-PEO block copolymers at silica. *Macromolecules* **1992**, *25*, 2474–2481.
- (16) Tiberg, F.; Malmsten, M.; Linse, P.; Lindman, B. Kinetic and equilibrium aspects of block copolymer adsorption. *Langmuir* **1991**, *7*, 2723–2730.
- (17) Himmelhaus, M.; Bastuck, T.; Tokumitsu, S.; Grunze, M.; Livadaru, L.; Kreuzer, H. J. Growth of a dense polymer brush layer from solution. *Europhys. Lett.* **2003**, *64*, 378–384.
- (18) Zdyrko, B.; Luzinov, I. Polymer brushes by the "grafting to" method. *Macromol. Rapid Commun.* **2011**, *32*, 859–869.
- (19) de Gennes, P. G. Polymers at an interface - a simplified view. *Adv. Colloid Interface Sci.* **1987**, *27*, 189–209.
- (20) de Gennes, P. G. Conformations of polymers attached to an interface. *Macromolecules* **1980**, *13*, 1069–1075.
- (21) Kingshott, P.; Thissen, H.; Griesser, H. J. Effects of cloud-point grafting, chain length, and density of PEG layers on competitive adsorption of ocular proteins. *Biomaterials* **2002**, *23*, 2043–2056.
- (22) Taylor, W.; Jones, R. A. L. Producing high-density high-molecular-weight polymer brushes by a "grafting to" method from a concentrated homopolymer solution. *Langmuir* **2010**, *26*, 13954–13958.
- (23) Taylor, W.; Jones, R. A. L. Protein adsorption on well-characterized polyethylene oxide brushes on gold: Dependence on molecular weight and grafting density. *Langmuir* **2013**, *29*, 6116–6122.
- (24) Nel, A. E.; Madler, L.; Velegol, D.; Xia, T.; Hoek, E. M. V.; Somasundaran, P.; Klaessig, F.; Castranova, V.; Thompson, M. Understanding biophysicochemical interactions at the nano-bio interface. *Nat. Mater.* **2009**, *8*, 543–557.
- (25) Herrwerth, S.; Eck, W.; Reinhardt, S.; Grunze, M. Factors that determine the protein resistance of oligoether self-assembled monolayers - Internal hydrophilicity, terminal hydrophilicity, and lateral packing density. *J. Am. Chem. Soc.* **2003**, *125*, 9359–9366.
- (26) Jung, L. S.; Campbell, C. T.; Chinowsky, T. M.; Mar, M. N.; Yee, S. S. Quantitative interpretation of the response of surface plasmon resonance sensors to adsorbed films. *Langmuir* **1998**, *14*, 5636–5648.
- (27) Prime, K. L.; Whitesides, G. M. Adsorption of proteins onto surfaces containing end-attached oligo(ethylene oxide) - a model system using self-assembled monolayers. *J. Am. Chem. Soc.* **1993**, *115*, 10714–10721.
- (28) Prime, K. L.; Whitesides, G. M. Self-assembled organic monolayers - model systems for studying adsorption of proteins at surfaces. *Science* **1991**, *252*, 1164–1167.
- (29) Lokanathan, A. R.; Zhang, S.; Regina, V. R.; Cole, M. A.; Ogaki, R.; Dong, M. D.; Besenbacher, F.; Meyer, R. L.; Kingshott, P. Mixed poly(ethylene glycol) and oligo(ethylene glycol) layers on gold as nonfouling surfaces created by backfilling. *Biointerphases* **2011**, *6*, 180–188.
- (30) Junesch, J.; Sannomiya, T.; Dahlin, A. B. Optical properties of nanohole arrays in metal-dielectric double films prepared by mask-on-metal colloidal lithography. *ACS Nano* **2012**, *6*, 10405–10415.
- (31) Mohsen-Nia, M.; Modarress, H.; Rasa, H. Measurement and modeling of density, kinematic viscosity, and refractive index for poly(ethylene glycol) aqueous solution at different temperatures. *J. Chem. Eng. Data* **2005**, *50*, 1662–1666.
- (32) Dahlin, A. B.; Mapar, M.; Xiong, K. L.; Mazzotta, F.; Hook, F.; Sannomiya, T. Plasmonic nanopores in metal-insulator-metal films. *Adv. Opt. Mater.* **2014**, *2*, 556–564.
- (33) de Feijter, J. A.; Benjamins, J.; Veer, F. A. Ellipsometry as a tool to study adsorption behavior of synthetic and biopolymers at air-water-interface. *Biopolymers* **1978**, *17*, 1759–1772.
- (34) Voros, J. The density and refractive index of adsorbing protein layers. *Biophys. J.* **2004**, *87*, 553–561.
- (35) Bailey, F. E.; Callard, R. W. Some properties of poly(ethylene oxide) in aqueous solution. *J. Appl. Polym. Sci.* **1959**, *1*, 56–62.
- (36) Oesterhelt, F.; Rief, M.; Gaub, H. E. Single molecule force spectroscopy by AFM indicates helical structure of poly(ethylene glycol) in water. *New J. Phys.* **1999**, *1*.
- (37) Ataman, M. Properties of aqueous salt-solutions of poly(ethylene oxide) - cloud points, theta-temperatures. *Colloid Polym. Sci.* **1987**, *265*, 19–25.
- (38) Florin, E.; Kjellander, R.; Eriksson, J. C. Salt effects on the cloud point of the poly(ethylene oxide) + water-system. *J. Chem. Soc., Faraday Trans I* **1984**, *80*, 2889–2910.
- (39) Zhang, Y. J.; Furyk, S.; Bergbreiter, D. E.; Cremer, P. S. Specific ion effects on the water solubility of macromolecules: PNIPAM and the Hofmeister series. *J. Am. Chem. Soc.* **2005**, *127*, 14505–14510.
- (40) Thormann, E. On understanding of the Hofmeister effect: How addition of salt alters the stability of temperature responsive polymers in aqueous solutions. *RSC Adv.* **2012**, *2*, 8297–8305.
- (41) Lee, H. S.; Penn, L. S. Evidence for relative radius of gyration as the criterion for selective diffusion behavior of polymer brushes. *Langmuir* **2009**, *25*, 7983–7989.
- (42) Reviakine, I.; Johannsmann, D.; Richter, R. P. Hearing what you cannot see and visualizing what you hear: Interpreting quartz crystal microbalance data from solvated interfaces. *Anal. Chem.* **2011**, *83*, 8838–8848.
- (43) Squires, T. M.; Messinger, R. J.; Manalis, S. R. Making it stick: convection, reaction and diffusion in surface-based biosensors. *Nat. Biotechnol.* **2008**, *26*, 417–426.
- (44) Vericat, C.; Vela, M. E.; Benitez, G.; Carro, P.; Salvarezza, R. C. Self-assembled monolayers of thiols and dithiols on gold: New

challenges for a well-known system. *Chem. Soc. Rev.* **2010**, *39*, 1805–1834.

(45) Nuzzo, R. G.; Zegarski, B. R.; Dubois, L. H. Fundamental studies of the chemisorption of organosulfur compounds on Au(111) - implications for molecular self-assembly on gold surfaces. *J. Am. Chem. Soc.* **1987**, *109*, 733–740.

(46) Schoch, R. L.; Kapinos, L. E.; Lim, R. Y. H. Nuclear transport receptor binding avidity triggers a self-healing collapse transition in FG-nucleoporin molecular brushes. *Proc. Natl. Acad. Sci. U.S.A.* **2012**, *109*, 16911–16916.

(47) Schoch, R. L.; Lim, R. Y. H. Non-interacting molecules as innate structural probes in surface plasmon resonance. *Langmuir* **2013**, *29*, 4068–4076.

(48) Peterlinz, K. A.; Georgiadis, R. Two-color approach for determination of thickness and dielectric constant of thin films using surface plasmon resonance spectroscopy. *Opt. Commun.* **1996**, *130*, 260–266.

(49) Lim, R. Y. H.; Deng, J. Interaction forces and reversible collapse of a polymer brush-gated nanopore. *ACS Nano* **2009**, *3*, 2911–2918.

(50) Kienberger, F.; Pastushenko, V. P.; Kada, G.; Gruber, H. J.; Riener, C.; Schindler, H.; Hinterdorfer, P. Static and dynamical properties of single poly(ethylene glycol) molecules investigated by force spectroscopy. *Single Mol.* **2000**, *1*, 123–128.

(51) Lee, H.; Venable, R. M.; MacKerell, A. D.; Pastor, R. W. Molecular dynamics studies of polyethylene oxide and polyethylene glycol: Hydrodynamic radius and shape anisotropy. *Biophys. J.* **2008**, *95*, 1590–1599.

(52) Mark, J. E.; Flory, P. J. The configuration of the polyoxyethylene chain. *J. Am. Chem. Soc.* **1965**, *87*, 1415–1423.

(53) Rahme, K.; Chen, L.; Hobbs, R. G.; Morris, M. A.; O'Driscoll, C.; Holmes, J. D. PEGylated gold nanoparticles: Polymer quantification as a function of PEG lengths and nanoparticle dimensions. *RSC Adv.* **2013**, *3*, 6085–6094.

(54) Pasche, S.; De Paul, S. M.; Voros, J.; Spencer, N. D.; Textor, M. Poly(L-lysine)-graft-poly(ethylene glycol) assembled monolayers on niobium oxide surfaces: A quantitative study of the influence of polymer interfacial architecture on resistance to protein adsorption by ToF-SIMS and in situ OWLS. *Langmuir* **2003**, *19*, 9216–9225.

(55) Satomi, T.; Nagasaki, Y.; Kobayashi, H.; Otsuka, H.; Kataoka, K. Density control of poly(ethylene glycol) layer to regulate cellular attachment. *Langmuir* **2007**, *23*, 6698–6703.

(56) Unsworth, L. D.; Sheardown, H.; Brash, J. L. Polyethylene oxide surfaces of variable chain density by chemisorption of PEO-thiol on gold: Adsorption of proteins from plasma studied by radiolabelling and immunoblotting. *Biomaterials* **2005**, *26*, 5927–5933.

(57) Unsworth, L. D.; Sheardown, H.; Brash, J. L. Protein resistance of surfaces prepared by sorption of end-thiolated poly(ethylene glycol) to gold: Effect of surface chain density. *Langmuir* **2005**, *21*, 1036–1041.

(58) Satulovsky, J.; Carignano, M. A.; Szleifer, I. Kinetic and thermodynamic control of protein adsorption. *Proc. Natl. Acad. Sci. U.S.A.* **2000**, *97*, 9037–9041.

(59) Tagliazucchi, M.; Szleifer, I. Stimuli-responsive polymers grafted to nanopores and other nano-curved surfaces: Structure, chemical equilibrium and transport. *Soft Matter* **2012**, *8*, 7292–7305.

(60) Larson-Smith, K.; Pozzo, D. C. Competitive adsorption of thiolated poly(ethylene glycol) and alkane-thiols on gold nanoparticles and its effect on cluster formation. *Langmuir* **2012**, *28*, 13157–13165.